J. Shanghai Jiao Tong Univ. (Sci.), 2019, 24(2): 262-272
https://doi.org/10.1007/s12204-018-1995-9

Optimization of Clinching Tools by Integrated Finite Element Model and Genetic Algorithm Approach

WANG Menghan∗ (王梦寒), *XIAO Guiqian* (肖贵乾), *WANG Jinqiang* (王晋强), *LI Zhi* (李　志)
(College of Materials Science and Engineering, Chongqing University, Chongqing 400044, China)

Abstract: Clinching is a convenient and efficient cold forming process that can join two sheets without any additional part. This study establishes an intelligent system for optimizing the clinched joint. Firstly, a mathematical model which introduces the ductile damage constraint to prevent cracking during clinching process is proposed. Meanwhile, an optimization methodology and its corresponding computer program are developed by integrated finite element model (FEM) and genetic algorithm (GA) approach. Secondly, Al6061-T4 alloy sheets with a thickness of 1.4 mm are used to verify this optimization system. The optimization program automatically acquires the largest axial strength which is approximately equal to 872 N. Finally, sensitivity analysis is implemented, in which the influence of geometrical parameters of clinching tools on final joint strength is analyzed. The sensitivity analysis indicates the main parameters to influence joint strength, which is essential from an industrial point of view.
Key words: mechanical clinching, optimization design, genetic algorithm (GA), ductile damage
CLC number: TG 938　　**Document code:** A

0 Introduction

Clinching is a convenient and cheap mechanical process which makes it more and more attractive for many applications such as automobile parts, agricultural apparatus and household electric appliances. However, there are many factors to limit the use of the clinching technology. One of the most important factors is joint strength. Therefore, the primary task is to design a clinching tool which can acquire a clinched joint with the biggest strength. There are many methods to design clinching tools. Numerical simulation is gradually used to investigate clinching process. For example, Varis and Lepist[1] investigated the suitability of numerical simulation for clinching process. The numerical simulation can reduce the amount of testing, but the testing cannot be fully eliminated since some verifications have been always needed to assure the correctness of the results. Hamel et al.[2] developed a 2D axisymmetric model of joining process, using a re-meshing procedure to deal with the large deformation. The results show that numerical simulation is appropriate for estimating the feasibility of clinching process, and it is also suitable for further investigating the influence of tools' geometry on final joint geometry. Coppieters et al.[3-4] conducted the comparison between experimental and numerical results. These results indicate that numerical simulation is very effective to reproduce the clinching process. However, these numerical simulations do not consider material damage. Lambiase and Ilio[5] developed a numerical model describing the evolution of the ductile damage to predict the onset of fracture.

Some scholars turned their attention to strength optimization. For instance, Coppieters et al.[6] investigated the possibility of predicting shear and pull-out strength of a sheet metal assembly using finite element model (FEM). According to their investigation, shear and pull-out strength of clinched joint can be accurately calculated by FEM but it is very time-consuming. Moreover, Oudjene and Ben-Ayed[7] investigated the effects of tools' geometry on feature parameters of clinched joint. In that study, the method for Taguchi's design of experiments (DoE) was used to optimize joint strength. In order to further optimize the strength, researchers introduced many optimization measures in numerical simulation field as the control method to seek out the best combination of process parameters. For instance, an optimization model of clinching tools, based on artificial intelligence techniques and FEM, was developed by Lambiase and Ilio[8]. In that model, the effect of process parameters on joint strength was calculated by

Received date: 2017-04-05
Foundation item: the Fundamental Research Funds for the Central Universities of China (No. CDJZR14130006)
∗**E-mail:** cquwmh@163.com

finite element simulation, and the joint characteristic under different processing conditions was predicted by artificial neural network (ANN). Hence, the joint strength has been optimized by integrating optimization algorithm and ANN approach. Roux and Bouchard[9] optimized a clinched joint using the optimization algorithm based on Kriging meta-model. The mechanical strength of the clinched joint has been increased by 13.5%. Sun and Khaleel[10] performed an optimization of the self-piercing rivets through analyzing rivet strength estimation. Oudjene et al.[11] optimized the clinching tools by means of response surface methodology (RSM) combined with moving least-square approximation and Taguchi method. Lebaal et al.[12] proposed a modified Kriging meta-model. The use of the Kriging meta-model is an effective way to improve the convergent performance.

However, almost all of the studies have used an approximate method (RSM, ANN, and Kriging meta-model) to obtain the relationship between design variables and design objective rather than using direct communication between FEM and optimization algorithm. Global optimization solution is lost easily via approximate methods, because the complicated relationship usually cannot be accurately approximated, especially for those multi-parameters' clinching process. In this study, a dynamic optimization system based on direct communication between FEM and genetic algorithm (GA) is proposed. The system is applied to identify the best geometric parameters of clinching tools without any manual intervention. The optimization results indicate that the optimization method based on direct communication has a good feasibility and robustness.

1 Optimization Model for Joint Strength

A clinched joint is easy to be failure under an axial load. In other words, axial strength is a weak aspect, compared with shear strength[7,11,13]. Therefore, the axial strength of the clinched joint is mainly discussed.

1.1 Analytical Formula

Typical joint failure modes in axial direction are button separation and neck fracture, as shown in Figs. 1(a) and 1(b). The joint strength in axial direction can be calculated by numerical simulation as well as by analytical formula. Considering accuracy and time cost, analytical formula based on Tresca yield criterion has been developed to calculate axial joint strength. A clinched joint is characterized by the following parameters: neck thickness (t_n), interlocking length (t_u), inner diameter (d) and inclination angle (θ), as shown in Fig. 1(c). In fact, joint strength can be defined as a function of t_n, t_u, d and θ.

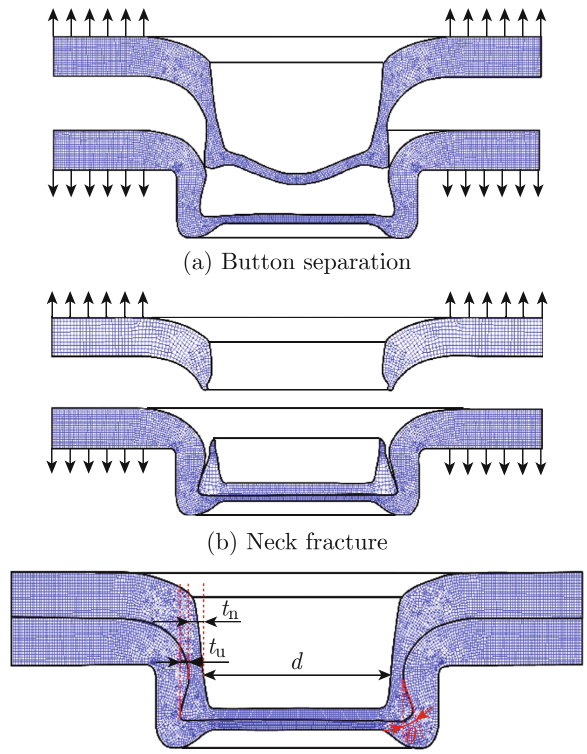

(a) Button separation

(b) Neck fracture

(c) Feature parameters

Fig. 1 Two basic failure modes and feature parameters

1.1.1 *Button Separation Mode*

Button separation mode is the separation of upper sheet and lower sheet due to insufficient geometrical interlocking (Fig. 1(a)). Under axial loading, the upper sheet is separated vertically from the locking location to the outside of the joint. The analytical formula for calculating the separation load is[3]

$$F_s = \frac{\pi}{4}\sigma_s[(d+2t_n)^2 - d^2]\frac{\tan\theta + u}{u}\tilde{t}, \qquad (1)$$

where

$$\tilde{t} = 1 - \left[\frac{(d+t_n)t_n}{(d+t_n+t_u)(t_n+t_u)}\right]^{\frac{u}{\tan\theta}},$$

σ_s is the critical failure strength of the upper sheet, u is the frictional coefficient between upper sheet and lower sheet, and F_s represents the axial virtual strength of the button separation mode. Other parameters have been illustrated in Fig. 1(c). According to elasticity theory, the equivalent stress of the joined component must be not more than the initial yield strength. Thus, σ_s is assigned as the initial yield strength of the upper sheet to ensure the safety of the joint during the period of service.

1.1.2 *Neck Fracture Mode*

Neck fracture mode is a failure of mechanically clinched joint by fracture of the upper sheet in the thin neck, as shown in Fig. 1(b). Obviously, the joint strength of this failure mode is equal to the product of the cross-sectional area and the tensile strength of joint material. Therefore, the calculating formula is

$$F_f = \sigma_s S = \frac{\pi}{4}\sigma_s[(d + 2t_n)^2 - d^2], \quad (2)$$

where S is the area of neck region, and F_f represents the axial virtual strength for the neck fracture mode. According to elasticity theory, the equivalent stress of the joined component must be less than or equal to the initial yield strength. Thus, σ_s is assigned as the initial yield strength of the upper sheet to ensure the safety of the joint without any plastic deformation during the period of service.

1.2 Optimization Model

1.2.1 *Objective Function*

The real strength of clinched joint in axial direction is

$$F = \min(F_f, F_s). \quad (3)$$

The reason is that only one failure mode is triggered in axial loading. In order to understand the relationship between two kinds of failure modes easily, the virtual and real strength surfaces for two failure modes are displayed in Figs. 2(a) and 2(b), respectively.

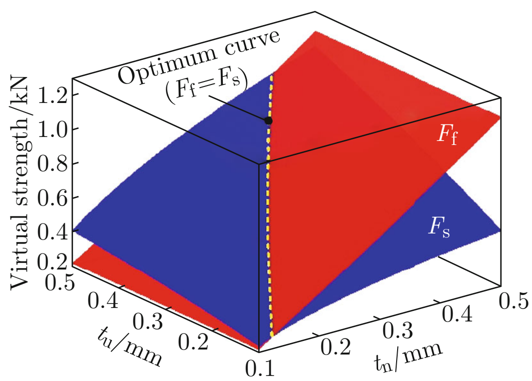

(a) Virtual strength surface

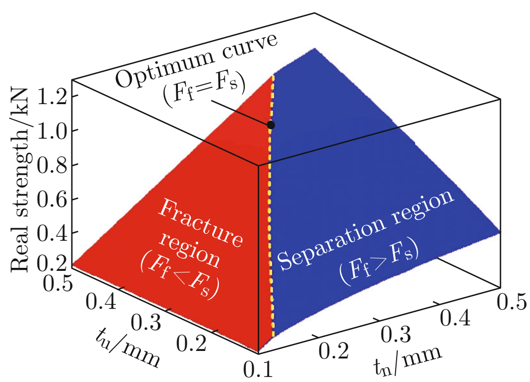

(b) Real strength surface

Fig. 2 Virtual and real strength surfaces for two basic modes ($u = 0.3$, $d = 4$ mm)

The surface of F_f, a quadric surface, is very approximate to a plane. The surface of F_s is a complicated and arched surface (Fig. 2(a)). The intersecting curve between two surfaces is the optimum curve at $F_f = F_s$, as shown in Fig. 2. It is extremely difficult or even impossible to make t_n and t_u reach a big value synchronously. Due to the intricate relationship between joint's shape and tools' shape, t_n and t_u cannot be directly controlled.

The goal of this study is to maximize F. Therefore, the objective function can be defined by

$$F_{max} = \max(\min(F_f, F_s)), \quad (4)$$

where F_{max} is the maximal real strength. As deduced in Subsection 1.1, F_f and F_s are defined as the functions of the joint feature parameters, such as t_n, t_u and θ. However, the design variables cannot be defined as t_n, t_u and θ. The reason is that the controllable parameters are not the feature parameters of clinched joint but the geometry parameters of clinching tools, such as $\{x_1, x_2, \cdots, x_{12}\}$, as illustrated in Fig. 3. According to Ref. [14], the main factor affecting the mechanical properties of clinched joint is the geometrical parameters of clinching tools. In fact, t_n, t_u and θ are the intricately unknown functions of $\{x_1, x_2, \cdots, x_{12}\}$. Fortunately, these functions can be determined by FEM.

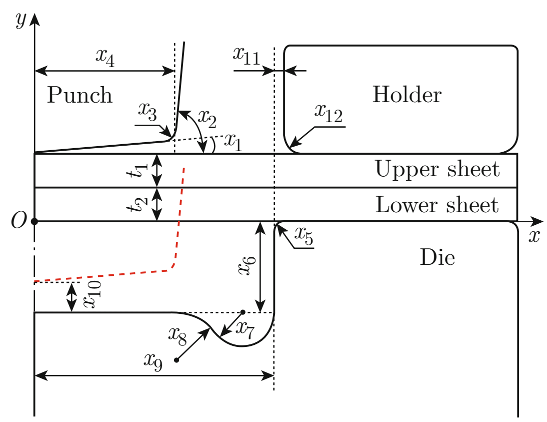

Fig. 3 Schematic representation of clinching tools with geometry parameters

1.2.2 *Constraint Conditions*

In order to improve the efficiency of the optimization algorithm, the feasible region of the design variables should be defined as

$$B_L \leqslant \{x_1, x_2, \cdots, x_{12}\} \leqslant B_U, \quad (5)$$

where B_L and B_U are the upper and lower boundaries, respectively.

In many applications, the upper surface of the joint is used as the functional surface which requires that the surface should not be convex[15]. Hence, the joint shape illustrated in Fig. 4(a) is the undesirable joint.

The constraint of the joint shape should be adopted to acquire the perfect joint, as shown in Fig. 4(b), and this shape constraint is

$$h \leqslant 0, \tag{6}$$

where h is also a function of the geometry parameters of clinching tools.

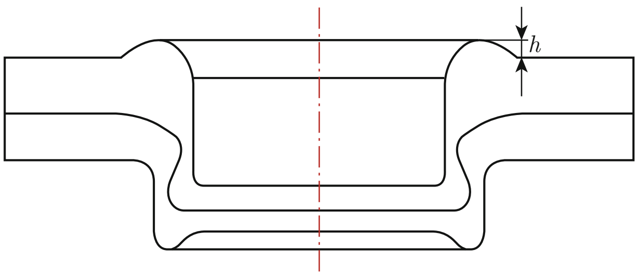

(a) Bad joint

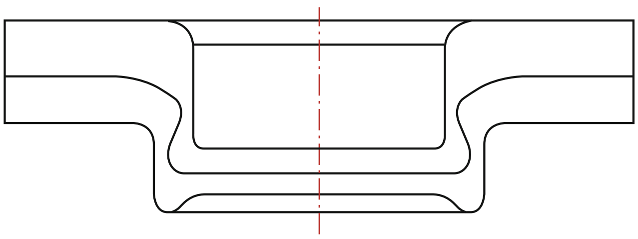

(b) Perfect joint

Fig. 4 Shape constraint of clinched joint

The most important constraint is the damage constraint. In order to obtain high-integrity joint, the damage of material must be limited. Otherwise, the fracture of the joint may take place in the clinching process. Therefore, the damage constraint is

$$D = \int_0^{\bar{\varepsilon}_\mathrm{f}} \frac{\sigma^*}{\bar{\sigma}} \mathrm{d}\bar{\varepsilon} \leqslant C, \tag{7}$$

where C is the damage threshold, D is the damage value of clinching material, $\bar{\varepsilon}$ is the equivalent strain, $\bar{\sigma}$ is the equivalent stress, σ^* is the maximum tensile stress at material fracture, and $\bar{\varepsilon}_\mathrm{f}$ is the equivalent strain of material fracture. Hambli and Reszka[16] used inverse technique method to identify suitable fracture criteria in blanking experiments. The purpose of this constraint is to ensure that high-integrity joint can be acquired in the optimization process.

1.2.3 *Mathematical Optimization Model*

The optimization model for the strength of clinched joint can be established as

$$\min(-\min(F_\mathrm{f}, F_\mathrm{s})), \tag{8}$$

which is subject to $\{t_\mathrm{n}, t_\mathrm{u}, \theta, d, h, D\} = \mathrm{FEM}(x_1, x_2, \cdots, x_{12})$, Eq. (1), Eq. (2), Eq. (5), Eq. (6) and Eq. (7). Here, FEM includes numerical simulation submodule and feature extraction sub-module. These modules will be discussed in the next section. In fact, σ_s does not affect the optimization process, because it is shared by F_f and F_s.

2 Solution Strategy For Optimization Model

The purpose of the optimization model is to seek out a combination of clinching tools such that it can obtain the strongest joint. There are many algorithms which have been developed to solve this type of problem, such as simulated annealing algorithm (SAA), particle swarm optimization (PSO) and GA.

2.1 Algorithm Structure

It is very easy for GA to obtain the optimization solution in global design space without any understanding of the relationship between objective value and design variables. In order to solve this complex minimization problem defined in Eq. (8), GA module and strength calculation module have been developed. In the previous studies, Roux and Bouchard[9] used ANN to replace the finite element simulation module. Lebaal et al.[12] employed RSM to replace the simulation module. However, the more accurate way to obtain the relationship between clinched joint and clinching tool is FEM.

The algorithm structure consists of two main modules which are GA module and fitness calculation module, as shown in Fig. 5, where T_1 and T_2 are the previously set thresholds, and F_i is the mechanical strength of the modified configuration using the parameter x_i. The process of fitness calculation is divided into two stages which are forming stage (I, II) and strength calculation stage (III). FEM has been adopted to simulate forming process in forming stage, and analytic formula has been used in strength calculation stage. There are several sub-modules in fitness calculation module, such as FEM sub-module (I), feature extraction submodule (II), strength calculation sub-module (III) and constraint sub-module (IV), as shown in Fig. 6.

Rational combination of fitness calculation module and GA module makes it possible to maximize axial strength of clinched joint without any manual intervention. The process of algorithm execution can be summarized as follows.

(1) GA module generates initial population, decodes gene of design variables and sends decoded design variables to fitness calculation module.

(2) CATIA V5R20 updates geometric model and outputs geometric model to Deform-2D. Deform-2D simulates clinching process and sends joint shape data to feature extraction sub-module.

(3) Feature extraction sub-module extracts $\{t_\mathrm{n}$, t_u, θ, h, $d\}$ and sends the feature parameters to strength calculation sub-module.

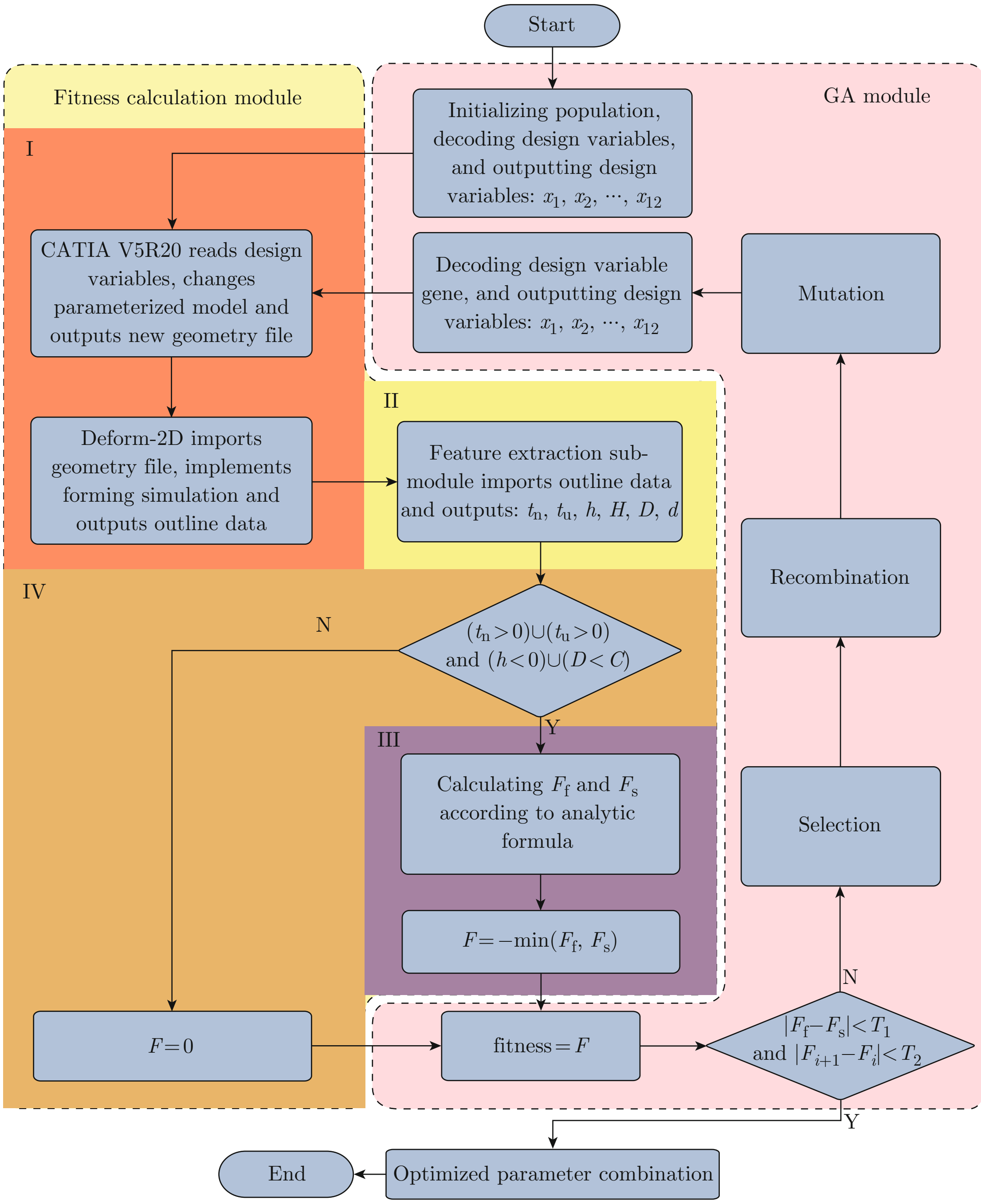

Fig. 5 Flow chart for optimizing joint strength

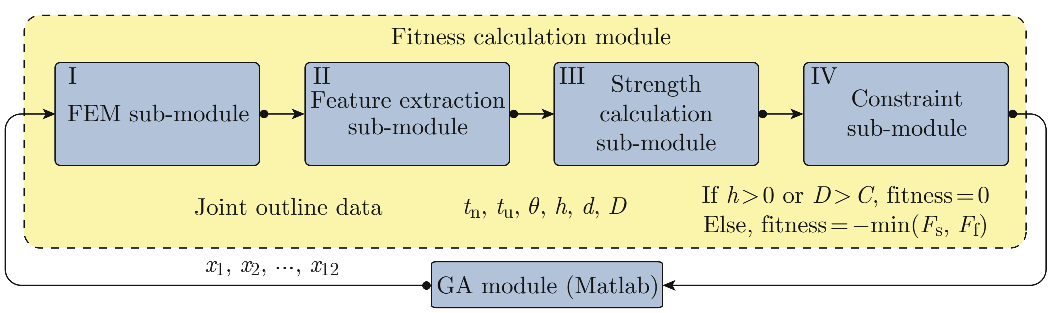

Fig. 6 The module of fitness calculation

(4) Strength calculation sub-module calculates F_f and F_s by analytic formula. If the calculation results meet the requirements of geometric constraint and damage constraint, $-\min(F_\mathrm{f}, F_\mathrm{s})$ is returned to GA module. Otherwise, zero is returned.

(5) GA module receives $-\min(F_\mathrm{f}, F_\mathrm{s})$ or zero as the fitness of individual. The individual with smaller fitness is reserved by GA module. Subsequently, the genes of the reserved individuals are recombined and mutated.

(6) If the solution has converged, the optimal solution is output and the optimizing process is terminated. Otherwise, it returns to Step (2).

2.2 FEM Sub-Module

The key technology of FEM sub-module is parametric simulation in which modeling and analysis can be applied automatically. A CATIA script based on Visual Basic is programed to realize the modeling. The parametric model of clinching tools is shown in Fig. 3. There are three tools, such as punch, holder and die. They are parameterized by $\{x_1, x_2, \cdots, x_{12}\}$, t_1 and t_2. In many applications, the thicknesses of upper sheet and lower sheet are given by manufacturers. Therefore, t_1 and t_2 cannot be appointed as the design variables. In this study, the design variables are $\{x_1, x_2, \cdots, x_{12}\}$, as illustrated in Fig. 3. In addition, fixed constraint in vertical direction has been applied to the holder. Hence, the location of the holder is unchanged in vertical direction during optimization process. Since the plastic forming process is a quasi-static process[17], a small loading speed should be used. Hence, a speed of 1 mm/s can be applied to the punch.

2.3 Feature Extraction Sub-Module

The core of feature extraction sub-module is feature extraction algorithm, in which the feature parameters $\{t_\mathrm{n}, t_\mathrm{u}, \theta, h, d\}$ can be calculated by the data of joint shape (Fig. 7(a)). The outline curve of upper sheet can be obtained from FEM sub-module. This outline curve, which is very similar to S-shape, cannot be defined as a function because there is no functional mapping relationship between x and y. Here, x and y are the coordinates of the point located in the S-shape curve. For example, for a given x-coordinate, there are many y-coordinates mapped to it and vice versa. In order to overcome this difficulty, v_i is introduced to build a functional mapping relationship, and it is defined as the arc length from the origin of the coordinate system to the given point (x_i, y_i):

$$v_i = \sum_{j=1}^{i} \sqrt{(x_j - x_{j-1})^2 + (y_j + y_{j-1})^2}. \tag{9}$$

Therefore, there is a functional mapping relationship between x_i and v_i as well as y_i and v_i. The x-coordinate of the outline curve for the upper sheet can increase, then decrease and then increase again from the coordinate origin to the right margin. This changed trend (red curve) is reflected in Fig. 7(b). However, the y-coordinate can decrease, and then increase.

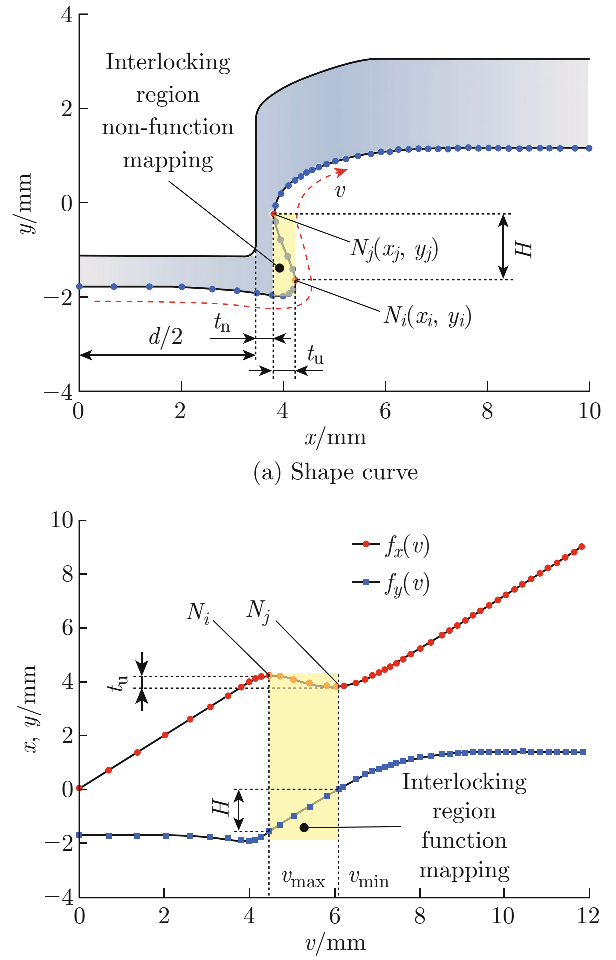

(a) Shape curve

(b) Parameterized curves

Fig. 7 Outline curve and its cumulative chord length parameterization curves

In order to obtain the feature parameters $\{t_\mathrm{n}$, t_u, θ, h, $d\}$ more accurately and quickly, B-Spline curve is employed to fit the point set (v_i, x_i) as well as the point set (v_i, y_i). Then, the parameterized equation is

$$\left.\begin{aligned} x &= f_x(v) \\ y &= f_y(v) \end{aligned}\right\}, \tag{10}$$

where, v is the introduced parameter; f_x and f_y are the functions determined by B-spline fitting method, as shown in Fig. 7(b). The points N_i and N_j must be obtained to calculate the feature parameters such as t_n, t_u, θ and d. It is difficult to extract N_i and N_j from Fig. 7(a). However, it is very easy to obtain N_i and N_j from Fig. 7(b). According to the theory of calculus, the extreme value points of N_i and N_j can be determined by $\mathrm{d}x/\mathrm{d}v = 0$. Substituting v_max and v_min into $f_y(v)$ can yield $f_y(v_\mathrm{max})$ and $f_y(v_\mathrm{min})$, respectively. On the basis of the above deductions, the calculation formula of the feature extraction algorithm can be developed as

$$\left.\begin{array}{l} \dfrac{\mathrm{d}x}{\mathrm{d}v} = 0 \Rightarrow v_{\max}, v_{\min} \\ t_{\mathrm{u}} = |f_x(v_{\max}) - f_x(v_{\min})| \\ \tan\theta = \dfrac{t_{\mathrm{u}}}{H} = \dfrac{|f_x(v_{\max}) - f_x(v_{\min})|}{|f_y(v_{\max}) - f_y(v_{\min})|} \\ t_{\mathrm{n}} = \left|f_x(v_{\min}) - \dfrac{d}{2}\right| \end{array}\right\}. \quad (11)$$

The formula can be used to extract the feature parameters from the shape data of clinched joint automatically.

3 Optimization Experiment

3.1 Model Definition

Al6061-T4 alloy sheets with a thickness of 1.4 mm are used in the optimizing process. The material properties are listed as follows: an elastic modulus of 68.9 GPa, a Poisson's ratio of 0.28, a yield stress of 168.1 MPa, a hardening law of $\bar{\sigma} = 538\bar{\varepsilon}^{0.172}$, and a critical damage of 1.61. The critical damage threshold of Al6061-T4 is 1.61[18]. The friction coefficient is assumed to be between 0.1 and 0.4[13-14].

In this study, the friction coefficient between tools and sheet is assumed as 0.1 and the friction coefficient between upper and lower sheets is assumed as 0.3. The number of individuals in each generation is set to 40, the crossover rate is set to 0.9, and the mutation rate is set to 0.1.

In order to increase the convergent rate and ensure that the crack does not occur for optimizing joint in the clinching process, the constraint condition is defined as

$$\left.\begin{array}{l} B_{\mathrm{L}} = \{0^\circ, 80^\circ, 0.1\,\mathrm{mm}, 2.7\,\mathrm{mm}, 0.1\,\mathrm{mm}, \\ \quad 1\,\mathrm{mm}, 0\,\mathrm{mm}, 4\,\mathrm{mm}, 3\,\mathrm{mm}, 0.6\,\mathrm{mm}, \\ \quad 0\,\mathrm{mm}, 0.1\,\mathrm{mm}\} \\ B_{\mathrm{U}} = \{10^\circ, 90^\circ, 0.6\,\mathrm{mm}, 3.8\,\mathrm{mm}, 0.5\,\mathrm{mm}, \\ \quad 2.5\,\mathrm{mm}, 2\,\mathrm{mm}, 6\,\mathrm{mm}, 5\,\mathrm{mm}, 1.4\,\mathrm{mm}, \\ \quad 5\,\mathrm{mm}, 1\,\mathrm{mm}\} \\ \qquad h \leqslant 0 \\ \qquad D \leqslant 1.61 \end{array}\right\}. \quad (12)$$

The initial population can be defined to reduce the computation time of the algorithm in practical application. However, in order to demonstrate the intelligence of the algorithm, the initial population has not been defined in this study.

3.2 Optimization Results and Discussion

In this study, the fitness is defined as the opposite of the axil joint strength. Then, the individual reserved in the last generation represents the optimized result. In order to understand evolutionary process clearly, the best individual at each generation is shown in Fig. 8, and the evolutionary curves are shown in Fig. 9.

Figure 8 shows the shapes of clinched joint after forming. The shape change of the joint is of great conspicuousness in the 1st, 2nd and 3rd generations, and it is very small after the fourth generation. This suggests that the joint shape has a big convergence rate in the former three generations. Moreover, the maximum damage of the sheets is far less than 1.61 of critical value at each generation. Therefore, the joint is not cracked in forming stage. The maximum damage is located in the lower right of the lower sheet, because the region is subjected to the tensile loads during forming process[5].

The strength of the joint gradually increases with the increase of the generation, and the convergence rate gradually decreases, because the search range is slowly near to the optimum individual. The objective function is not necessarily improved at each generation (Fig. 9(a)). This reason is that the optimization algorithm is global. Therefore, some computations are dedicated to the exploration of the design space. The optimization results also indicate that the feature extraction algorithm can automatically extract the feature parameters of the joint.

According to analytic formula, F_{s} and F_{f} can be calculated at each generation. The actual joint strength is equal to $\min(F_{\mathrm{s}}, F_{\mathrm{f}})$ which is the opposite of the fitness. The evolutionary relationship between two failure modes is illustrated in Fig. 9(b). In evolutionary process, F_{s} is always less than F_{f} and $|F_{\mathrm{f}} - F_{\mathrm{s}}|$ is very small (less than 40 N) at the 12th generation, which is consistent with the previous inference. This fact indicates that the global optimum solution has been obtained under certain tolerance.

The virtual strength distributions of two kinds of failure modes in some generations are demonstrated in Fig. 10. With the increase of the generation, the individuals are gradually gathered in a region of $F_{\mathrm{s}} = F_{\mathrm{f}}$. These evolution trends are controlled by previous corollary in which optimum solution should locate in a region of $F_{\mathrm{f}} = F_{\mathrm{s}}$ (Fig. 2).

Considering the cost of computation time and the optimization efficiency, the optimization program is terminated at the 12th generation although the joint strength can be further optimized. After 480 times of evolution, the optimized joint strength is approximately equal to 872 N and the optimized design variables are

$$\begin{array}{l} \{x_1, x_2, \cdots, x_{12}\} = \\ \quad \{0.91^\circ, 89.60^\circ, 0.17\,\mathrm{mm}, 3.22\,\mathrm{mm}, 0.23\,\mathrm{mm}, 1.58\,\mathrm{mm}, \\ \quad 0.59\,\mathrm{mm}, 1.67\,\mathrm{mm}, 4.98\,\mathrm{mm}, 0.66\,\mathrm{mm}, 0.29\,\mathrm{mm}, \\ \quad 0.79\,\mathrm{mm}\}. \end{array} \quad (13)$$

The feature parameter are $t_{\mathrm{n}} = 0.47\,\mathrm{mm}$, $t_{\mathrm{u}} = 0.33\,\mathrm{mm}$, and $\theta = 14.49^\circ$. All of these results prove that the optimization model is very reasonable to optimize the axial strength of clinched joint and the solving

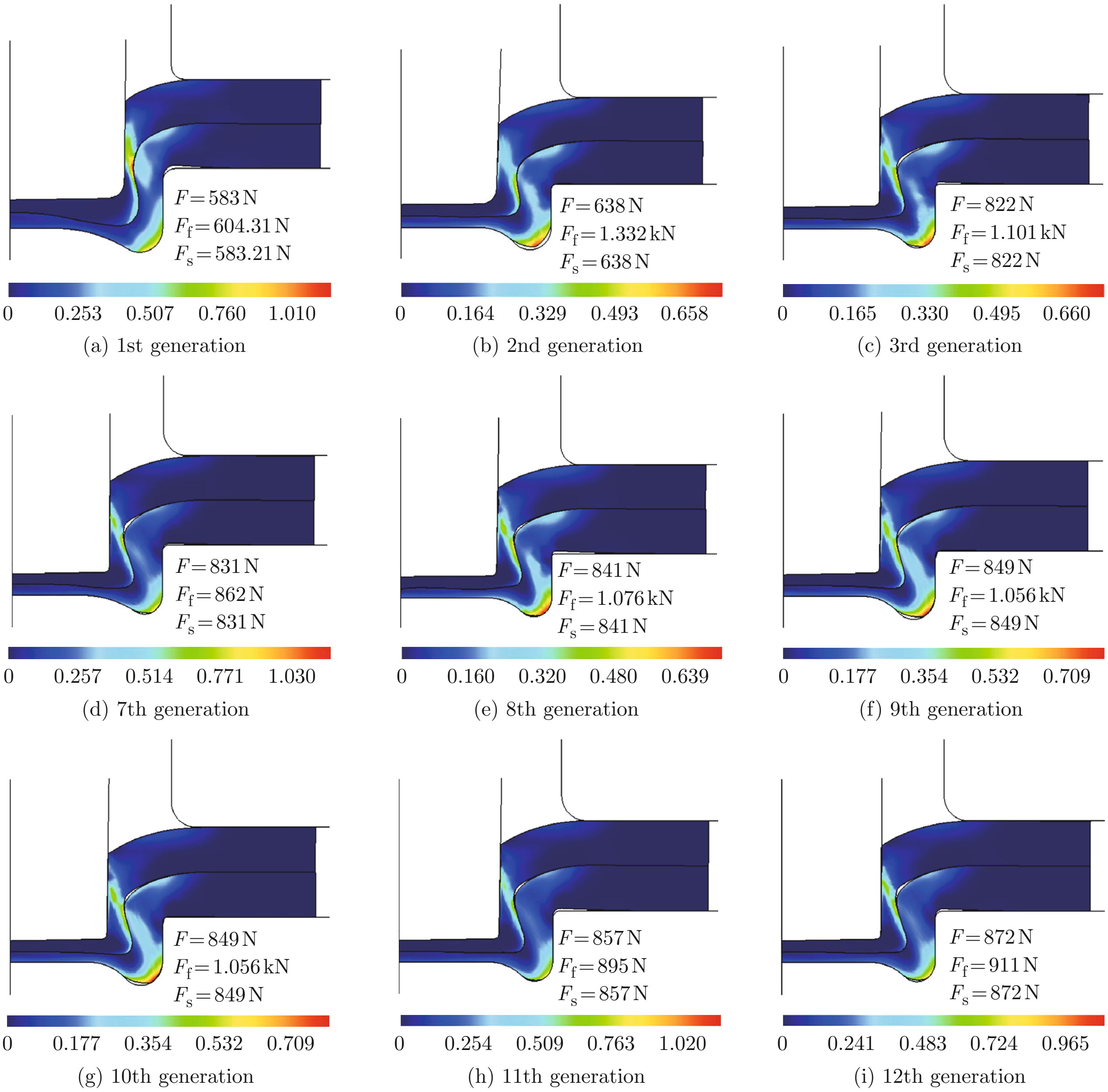

Fig. 8 Shape evolutionary of damage for the best individual at each generation

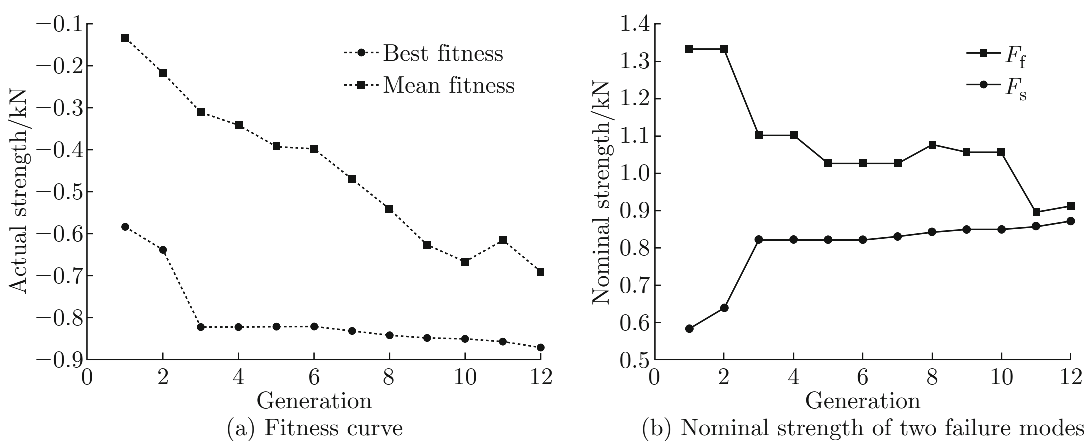

Fig. 9 Evolutionary curves for GA

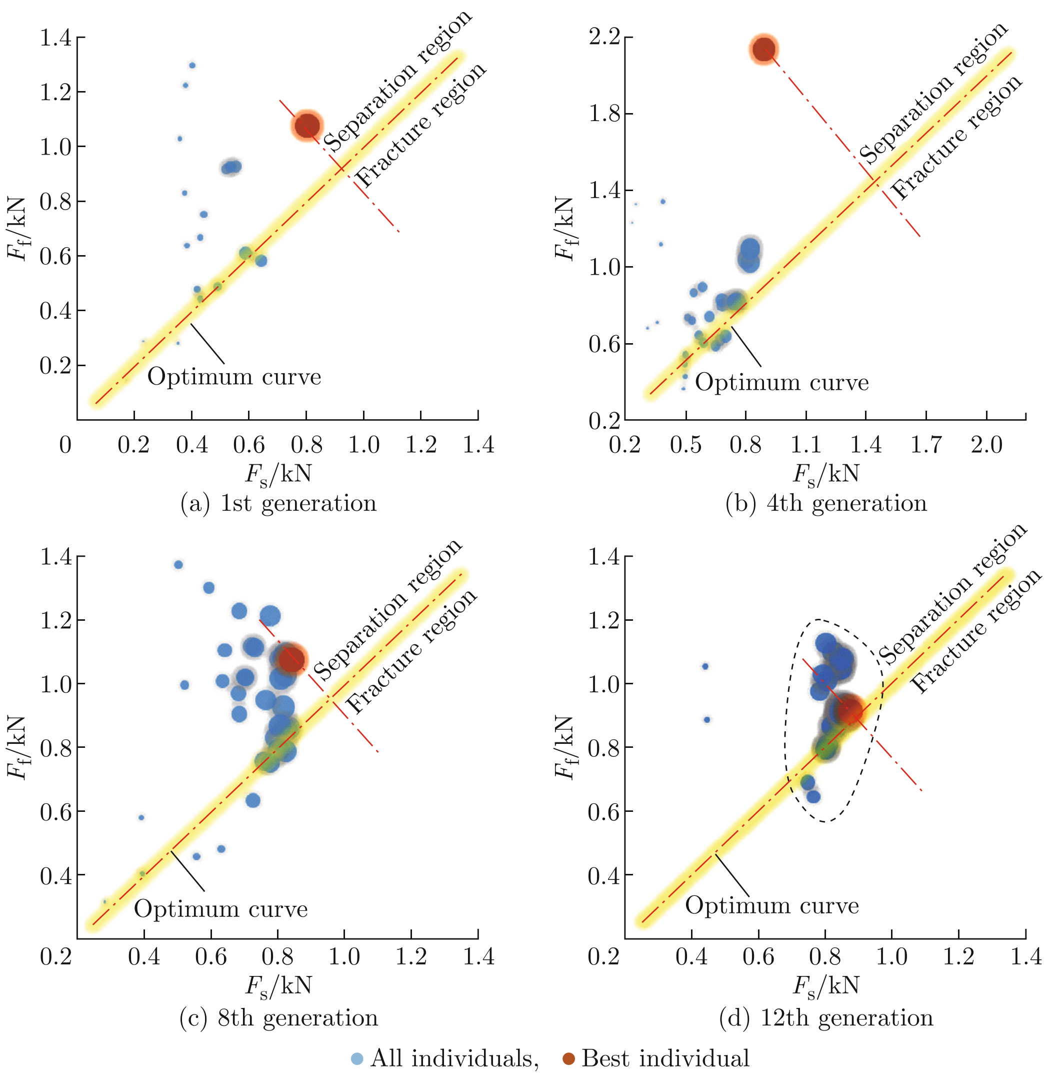

Fig. 10 Virtual strength distributions of two failure modes for all individuals

algorithm is suitable to solve this combination optimization problem.

3.3 Sensitivity Analysis

Although it is unnecessary to understand the relationship between joint strength and design variables in optimization process, the sensitivity analysis is implemented in this study to show which design variables having the main influence on joint strength, as well as to simplify the geometry parameters of clinching tools. The sensitivity (S_i) of each parameter is[9]

$$S_i = \frac{|F_i - F^{\text{ref}}|}{|x_i - x_i^{\text{ref}}|}\frac{x_i^{\text{ref}}}{F^{\text{ref}}}, \tag{14}$$

where x_i^{ref} is the reference value of each parameter, and F^{ref} is the mechanical strength of the reference configuration. In order to calculate the sensitivity of $x_i\,(i = 1, 2, \cdots, 12)$, the influence of other design variable $x_j\,(j \neq i; i = 1, 2, \cdots, 12)$ needs to be eliminated, so x_j and F^{ref} (872 N) should be assigned as the optimized values. The reason is that if $x_j\,(j \neq i; j = 1, 2, \cdots, 12)$ is assigned as the inappropriate value, F_i may be equal to zero although the change of x_i is very small or even without changing. Twelve simulations are performed to evaluate the sensitivity of each parameter. The twelve computations and the results are shown in Fig. 11.

Three important parameters are die radius (x_9), punch radius (x_4) and die depth (x_6). These parameters have a cumulative effect of more than 80% of the whole parameter sensitivity (Fig. 11). Moreover, gap between punch and die (x_{10}) and radius of die cavity (x_7) are also very important. The optimized parameters can be directly used in practical applications, the parameters $\{x_9, x_4, x_6, x_{10}, x_7\}$ can be first considered to simplify the tools' design and manufacturing, and the parameters $\{x_1, x_2, x_3, x_{11}\}$ can be ignored. The sensitivity analysis results are basically the same as those obtained from Ref. [9].

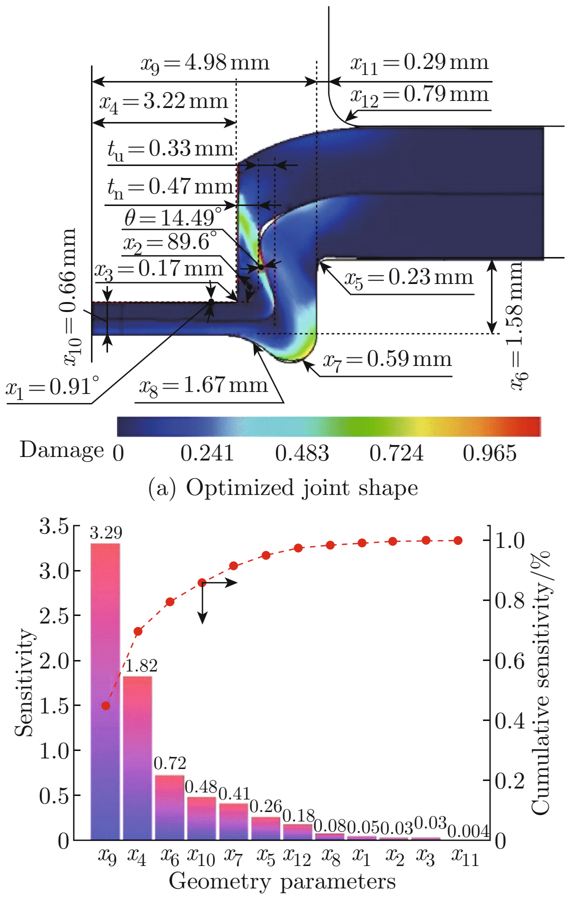

(a) Optimized joint shape

(b) Sensitivity analysis

Fig. 11 Optimized results and sensitivity analysis

3.4 Mechanism Analysis

The computation results show that the die radius and the punch radius are very important than other parameters. This is because d, t_n and t_u are determined directly by the die and punch radii. There is a relationship between these parameters:

$$x_9 = t_n + t_u + d + l, \tag{15}$$

where d is equal to x_4 when x_1 is close to zero and x_2 is close to 90°. This relationship is reflected in Fig. 12. According to the invariable volume theory, l is mainly determined by x_{10} and x_6 when x_9 and x_4 have been given.

Therefore, x_9, x_4, x_6 and x_{10} are the major parameters which determine the feature parameters of clinched joint. The change of x_7 has a small influence on the feature parameters, if it is sufficiently large. The reason is that x_7 affects the flow of material, and there is a positive correlation between the volume of die cavity and the volume of interlocking region (Fig. 12) when the volume of die is changed in a small range. On the contrary, the increase of the volume of interlocking region is limited when x_7 is very large. Hence, if x_7 is

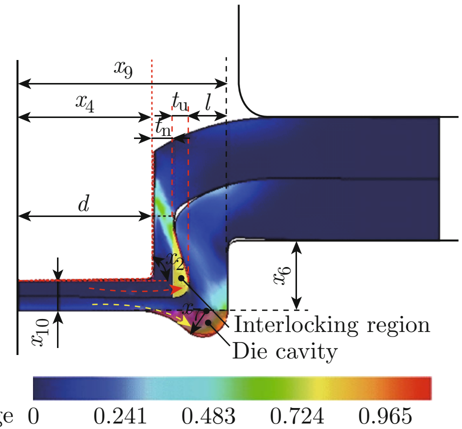

Fig. 12 Relationship between several key parameters

big enough, the influence of x_7 can be ignored. In conclusion, the influence of these parameters is interactive. The parameters $\{x_9, x_4, x_6, x_{10}\}$ are very important, x_7 should be given sufficiently, and other parameters can be ignored.

4 Conclusion

On the basis of FEM and GA, a global optimization methodology is developed to optimize joint strength. The optimized results verify the prediction of the optimization model.

(1) The optimization theory established in this study has a good feasibility to the optimization of joint strength. This optimization methodology can be applied to other optimization problems. The direct communication between FEM and optimization algorithm is a good way to acquire the correlation between design variables and design objective. According to this optimization methodology, an optimization system developed in this study can be directly applied to obtain the strongest joint and the corresponding tools without any manual intervention. This optimization method overcomes the shortcomings of approximate methods.

(2) The mechanical clinching technology has a great feasibility because the axial strength of clinched joint can reach 872 N. The optimization system established in this study can promote the use of the connection technology.

(3) The sensitivity analysis provides the best way to simplify the tools' structure. The parameters $\{x_5, x_{12}, x_8, x_1, x_2, x_3, x_{11}\}$ can be ignored, and other parameters should be assigned as the optimized values. The most important parameters are die radius (x_9) and punch radius (x_4), because these two parameters have a direct influence on neck thickness (t_n) and interlocking length (t_u). Moreover, die depth (x_6), gap between punch and die (x_{10}) and cavity radius of die (x_7) are also very important.

References

[1] VARIS J P, LEPISTÖ J. A simple testing-based procedure and simulation of the clinching process using finite element analysis for establishing clinching parameters [J]. *Thin-Walled Structures*, 2003, **41**(8): 691-709.

[2] HAMEL V, ROELANDT J M, GACEL J N, et al. Finite element modeling of clinch forming with automatic remeshing [J]. *Computers and Structures*, 2000, **77**(2): 185-200.

[3] COPPIETERS S, LAVA P, BAES S, et al. Analytical method to predict the pull-out strength of clinched connections [J]. *Thin-Walled Structures*, 2012, **52**(1): 42-52.

[4] COPPIETERS S, LAVA P, HECKE R V, et al. Numerical and experimental study of the multi-axial quasistatic strength of clinched connections [J]. *International Journal of Material Forming*, 2012, **6**(4): 437-451.

[5] LAMBIASE F, ILIO A D. Damage analysis in mechanical clinching: Experimental and numerical study [J]. *Journal of Materials Processing Technology*, 2016, **230**: 109-120.

[6] COPPIETERS S, COOREMAN S, LAVA P, et al. Reproducing the experimental pull-out and shear strength of clinched sheet metal connections using FEA [J]. *International Journal of Material Forming*, 2010, **4**(4): 429-440.

[7] OUDJENE M, BEN-AYED L. On the parametrical study of clinch joining of metallic sheets using the Taguchi method [J]. *Engineering Structures*, 2008, **30**(6): 1782-1788.

[8] LAMBIASE F, ILIO A D. Optimization of the clinching tools by means of integrated FE modeling and artificial intelligence techniques [J]. *Procedia CIRP*, 2013, **12**: 163-168.

[9] ROUX E, BOUCHARD P O. Kriging metamodel global optimization of clinching joining processes accounting for ductile damage [J]. *Journal of Materials Processing Technology*, 2013, **213**(7): 1038-1047.

[10] SUN X, KHALEEL M A. Performance optimization of self-piercing rivets through analytical rivet strength estimation [J]. *Journal of Manufacturing Processes*, 2005, **7**(1): 83-93.

[11] OUDJENE M, BEN-AYED L, DELAMÉZIÈRE A, et al. Shape optimization of clinching tools using the response surface methodology with moving least-square approximation [J]. *Journal of Materials Processing Technology*, 2009, **209**(1): 289-296.

[12] LEBAAL N, OUDJENE M, ROTH S. The optimal design of sheet metal forming processes: Application to the clinching of thin sheets [J]. *International Journal of Computer Applications in Technology*, 2012, **43**(2): 110-116.

[13] LEE C J, KIM J Y, LEE S K, et al. Design of mechanical clinching tools for joining of aluminium alloy sheets [J]. *Materials and Design*, 2010, **31**(4): 1854-1861.

[14] LEE C J, KIM J Y, LEE S K, et al. Parametric study on mechanical clinching process for joining aluminum alloy and high-strength steel sheets [J]. *Journal of Mechanical Science and Technology*, 2010, **24**(1): 123-126.

[15] GERSTMANN T, AWISZUS B. Recent developments in flat-clinching [J]. *Computational Materials Science*, 2014, **81**(2): 39-44.

[16] HAMBLI R, RESZKA M. Fracture criteria identification using an inverse technique method and blanking experiment [J]. *International Journal of Mechanical Sciences*, 2002, **44**(7): 1349-1361.

[17] CHEN C, ZHAO S D, HAN X L, et al. Optimization of a reshaping rivet to reduce the protrusion height and increase the strength of clinched joints [J]. *Journal of Materials Processing Technology*, 2016, **234**: 1-9.

[18] LEE C J, LEE J M, RYU H Y, et al. Design of hole-clinching process for joining of dissimilar materials Al6061-T4 alloy with DP780 steel, hot-pressed 22MnB5 steel, and carbon fiber reinforced plastic [J]. *Journal of Materials Processing Technology*, 2014, **214**(10): 2169-2178.